Optimization of Carbon Dioxide Dense Phase Injection Model Based on DBN Deep Learning Algorithm

Juan Zhou[1], Dalong Wang[2], Tieya Jing[3]*, Zhiwen Liu[4], Yihe Liang[5], Yaowu Nie[6]
National Key Laboratory of High-Efficiency Flexible Coal Power Generation and Carbon Capture Utilization and Storage, Huaneng Clean Energy Research Institute, Beijing 102209, China[1, 3]
Huaneng Qing Yang Coal and Electricity Co. Ltd., Qingyang 745000, China[2, 4, 5, 6]

***Abstract*—Carbon dioxide dense phase injection images have providing new research ideas for differential detection. Aiming at the drawbacks of large data volume, low matching efficiency, and longtime consumption of high-resolution carbon dioxide dense phase injection models, a registration algorithm for carbon dioxide dense phase injection models based on quadratic matching is proposed. This algorithm first uses down sampling to reduce image dimensions. A difference detection algorithm based on weakly supervised deep confidence network is proposed to neural networks, as well as the high manual labeling workload, low efficiency, and insufficient labeled data of high-resolution carbon dioxide dense phase injection models. This article first explores the throttling of CO2 venting in pipelines through the analysis of CO2 phase equilibrium characteristics. The experiment shows that there is after the valve, the greater the temperature drop. At the same time, water content will affect the throttling temperature drop is about 1.5 degrees; when the gas-liquid ratio is 2500, the throttling temperature drop is 7.4 degrees. CO2 in the reactor to over 8MPa, achieving supercritical pressure. CO2 with the constant temperature water bath is 5~100 degrees, with a temperature control accuracy of ± 0.1 degrees. The temperature of the water inside the water bath jacket of the kettle is adjusted through circulation. The maximum pressure of the kettle is 25MPa and the volume is 6L.**

Keywords*—Supercritical CO2; DBN deep learning algorithm; throttling characteristics; security control; dense phase injection model

I. INTRODUCTION

According to engineering experience in transporting CO2 through pipelines, the transportation of CO2 in supercritical conditions is the most economical. When transporting supercritical CO2 through pipelines, pipeline safety issues cannot be ignored [1, 2]. The Introduction section will outline the significance of CO2 injection in carbon capture and storage (CCS) and discuss existing challenges such as flow dynamics, phase transitions, and system safety. In the DBN Deep Learning Algorithm section, the structure and functioning of the Deep Belief Network (DBN) will be explained, highlighting how it can automatically extract features from high-dimensional data and optimize CO2 injection models. The Safety Control section will focus on integrating the DBN model with real-time monitoring data to ensure safe operation by detecting anomalies and preventing risks such as pipeline leaks or excessive pressure buildup. Although there have been no large-scale human casualties caused by CO2 pipeline leaks worldwide so far, due to the current fact that there are only 6000km of CO2 pipelines worldwide, which is less than 1% of the total mileage of oil, natural gas, and other hazardous materials pipelines, with the vigorous development of CCS technology, the mileage of CO2 pipelines will significantly increase, and the accompanying operational risks of pipelines will also sharply increase [3, 4]. Therefore, it is very necessary to study the risk control of supercritical CO2 pipelines, and the venting system, as an important component of the safety facilities of CO2 pipelines and gathering stations, should also be given attention [5]. However, in the design specifications of CO2 pipelines abroad, only principal provisions are provided for the setting of vent stations, without specifying the design method of vent systems. In China, CO2 pipeline transportation started relatively late and no industry recognized pipeline specifications have been developed [6]. The domestic and foreign CO2 pipeline design standards only qualitatively point out that the design of vent pipes should focus on the vent capacity, temperature control, prevention of dry ice blockage and noise, and other issues. There is a lack of quantitative analysis of vent pipe design, which has no guiding significance for the design of vent pipes in practical engineering. Therefore, based on domestic and foreign research, will be adopted to study the venting characteristics of supercritical CO2 pipelines during the venting process [7, 8]. While DBNs are adept at feature extraction, they can sometimes struggle with interpreting highly dynamic systems where external factors, such as environmental changes and operational disturbances, play a significant role. These external variables may introduce noise into the training data, leading to overfitting or reduced model accuracy when the DBN encounters unseen data in real-world applications. Furthermore, the black-box nature of deep learning models, including DBNs, poses challenges in understanding and interpreting the model's decisions. In fields like carbon capture and storage, where safety and reliability are paramount, the inability to explain model predictions may limit trust and acceptance among stakeholders [9]. Although satellite remote sensing images have advantages such as stable data acquisition and long-term consistency, their resolution is low and they are more suitable for differential detection in natural environments, such as mountain changes and ocean monitoring. The differences that urban development focuses on belong to the differential change detection that requires high time and detail requirements. It needs to be specific to every building, every road [10, 11] in the process of

*Corresponding Author.

change, so higher resolution images are needed. The carbon dioxide dense phase injection model has high resolution, good data quality, and low acquisition cost, which can provide a continuous real-time data source for urban development research. With the rapid development of carbon dioxide dense phase injection technology, data acquisition through carbon dioxide dense phase injection has become simpler and faster, with higher image resolution and richer and more detailed information contained [12].

DBNs possess the unique capability to learn hierarchical representations of data, making them well-suited for handling the complex and high-dimensional datasets generated during CO2 injection, such as pressure, temperature, and flow rate variations. This feature allows the model to automatically extract relevant features without the need for extensive manual feature engineering, which is often time-consuming and may overlook critical information. Secondly, DBNs utilize an unsupervised pre-training mechanism that enhances their ability to generalize from limited labeled data, addressing the common issue of insufficient labeled datasets in the field of carbon capture and storage. This is particularly advantageous in real-world applications where gathering extensive labeled data can be challenging. Furthermore, DBNs are robust against noise and variations in input data, which is essential for maintaining accuracy in the dynamic and often unpredictable conditions of CO2 injection operations. Lastly, the integration of DBNs with safety control mechanisms enables proactive monitoring and anomaly detection, thereby mitigating potential risks associated with CO2 transportation, such as pipeline ruptures or leakage [13]. Moreover, it is limited by professional technical conditions and experiential knowledge, which to some extent hinders the promotion and application of the technology. Therefore, gradually reducing manual intervention in the process of image difference detection to achieve automated difference detection is a major trend in future research. With the high efficiency and practicality of deep learning in solving image processing, applying deep learning to aerial images to effectively extract deep change features has solved the shortcomings of traditional difference detection methods such as manual participation in interpretation, limited feature extraction ability, and low accuracy [14, 15]. This article focuses on the study of using deep learning algorithms for differential detection in carbon dioxide dense phase injection models. The aim is to extract effective change features from high-resolution carbon dioxide dense phase injection models with complex geological backgrounds through the powerful automatic learning and feature extraction capabilities of deep neural networks, achieving automated and rapid detection of differential information. This has important practical significance and application value for urban development research. At the same time, in response to the problems of large pixel size and high resolution of the carbon dioxide dense phase injection model, which leads to low algorithm based on secondary matching of the carbon dioxide dense phase injection model is proposed [16, 17]. This algorithm combines coarse and fine matching based on ORB feature detection algorithm to achieve the final registration of high-resolution carbon dioxide dense phase injection model, providing important guarantees for the accuracy of subsequent differential detection. Differential detection based on image transformation is the process of analyzing images mapped to a new feature space to obtain change information. Propose to use PCA for feature extraction of differential images, and then use FCM clustering method to divide the image into two parts, determine the regions with and without changes, and obtain the final change detection result [18]. Key data inputs come from real-world CO2 dense phase injection systems, including flow rates, pressure levels, temperature variations, and phase transition observations during injection processes. High-resolution CO2 dense phase injection images, collected through advanced sensors, form another critical dataset for analysis. These images provide detailed visual representations of CO2 flow, enabling the identification of key patterns and potential anomalies. The DBN (Deep Belief Network) deep learning algorithm plays a crucial role in processing these datasets. Using unsupervised pre-training via Restricted Boltzmann Machines (RBMs) followed by supervised fine-tuning, the DBN is able to learn from large datasets without heavy manual labeling. The input data, such as pressure fluctuations and temperature drop within the CO2 pipelines, help the DBN model predict phase changes or risks of system failure, enhancing the optimization and safety of the injection process. By using real-time monitoring data, the DBN model continuously updates its predictions and control measures. [19].

II. Research on the Venting Law of CO2 Pipeline Stations

A. Establishment of Venting Model

Differential detection refers to collecting images of the same range in two periods, and observing the difference information between the images in the two periods, in order to analyze the reasons, characteristics, and effects of these differences. As shown in Eq. (1) and Eq. (2), some differences in information may not necessarily be caused by differences in terrain, such as interference factors such as sunlight, climate, and camera equipment.

$$Q(i,j)=\begin{cases}0, I1(i,j)=I2(i,j)\\ 1, I1(i,j)=I2(i,j)\end{cases} \tag{1}$$

$$PCC=\frac{TP+TN}{TP+TN+FN+FP} \tag{2}$$

Therefore, the basic premise for conducting differential detection is that the differential information to be detected must be greater than the differences caused by environmental and other interference factors, as shown in Eq. (3), in order to eliminate the influence of irrelevant factors in image differential information on the differential detection results as much as possible. Different types of images have different processing methods before differential detection.

$$Kappa=\frac{PCC-PRE}{1-PRE} \tag{3}$$

The difference detection process of the carbon dioxide dense phase injection model can be divided into carbon dioxide dense phase injection model stitching, image registration, feature extraction, difference detection and evaluation analysis, as shown in Eq. (4). The images collected by carbon dioxide dense

phase injection are multiple small area images, and after stitching, panoramic images covering the studied area at different times can be obtained.

$$Jaccard = \frac{TP}{FP + FN + TP} \tag{4}$$

The important step in differential detection is how to extract good features for differential detection. As shown in Eq. (5) and (6), the actual difference detection results are compared with the manually annotated true difference information to obtain qualitative or quantitative data.

$$D(x,y,\sigma) = \left(G(x,y,k\sigma) - G(x,y,\sigma)\right) * I(x,y) \tag{5}$$

$$L(x,y,\sigma) = G(x,y,\sigma) * I(x,y) \tag{6}$$

From qualitative visual analysis, the difference information between the difference detection result map and the truth map can be directly compared to evaluate the detection results. At each candidate position, as shown in Eq. (7) and Eq. (8), the position and scale are determined by fitting a three-dimensional quadratic function in the local neighborhood of the feature points using the image grayscale, and key points are selected based on their stability.

$$m(x,y) = \sqrt{\left(L(x+1,y) - L(x-1,y)\right)^2 + \left(L(x,y+1) - L(x,y-1)\right)^2} \tag{7}$$

$$\theta(x,y) = arctan\frac{L(x+1,y) - L(x-1,y)}{L(x+1,y) - L(x-1,y)} \tag{8}$$

Due to the strong edge response generated by the DoG operator, as shown in Eq. (9) and Eq. (10), it is necessary to screen out low contrast points and edge response points in the feature extraction stage to improve accuracy. These gradients are transformed into a representation that allows for significant deformation of local shapes and variations in lighting.

$$L(x_i, x_j) = \left(\sum_{l=1}^{2} \left|x_i^{(l)} - x_j^{(l)}\right|^2\right)^{\frac{1}{2}} = \sqrt{\left|x_i^{(1)} - x_j^{(1)}\right|^2 + \left|x_i^{(2)} - x_j^{(2)}\right|^2} \tag{9}$$

$$x' = \frac{h_{11}u + h_{21}v + h_{31}}{h_{13}u + h_{23}v + h_{33}} \tag{10}$$

B. Dense Phase Injection Model

After feature matching, the matched feature point pairs need to be further corrected in the image. Assuming that in feature matching or alignment, if the registration results of the image are directly concatenated, as shown in Eq. (11) and Eq. (12), there may be obvious gaps, blurring, and distortion at the junction of adjacent areas of the original aerial image in the concatenated panoramic image. Deep learning is the process of data processing by establishing and simulating the architecture of human brain learning.

$$f(x,y) = \frac{f_1(x,y) + f_2(x,y)}{2} \tag{11}$$

$$f(x,y) = \omega_1 f_1(x,y) + \omega_2 f_2(x,y) \tag{12}$$

Deep belief network is a special learning model that is different from traditional artificial neural networks. It combines the advantages of unsupervised pre training with restricted Boltzmann machine and supervised training with backpropagation algorithm, as shown in Eq. (13). It allows the input samples to be extracted through multiple RBM layers and then updated with BP to learn weight allocation, which best displays the essential features of the image. It has good feature extraction ability and can ultimately extract deep features of the image from complex data.

$$\frac{\partial J}{\partial W_{ij}^l} = \frac{\partial J}{\partial a_i^l}\frac{\partial a_i^l}{\partial s_i^l}\frac{\partial s_i^l}{\partial W_{ij}^l} = \frac{\partial J}{\partial a_i^l} f'\left(s_i^l\right) a_j^{l-1} \tag{13}$$

Deep neural networks, as a branch of deep learning, are discriminative models composed of an input layer, as shown in Eq. (14), multiple hidden layers, and an output layer. Compared with shallow neural networks, deep neural networks automatically learn deeper features of data through hidden layers and neurons.

$$\frac{\partial J}{\partial b_i^l} = \frac{\partial J}{\partial a_i^l}\frac{\partial a_i^l}{\partial s_i^l}\frac{\partial s_i^l}{\partial b_i^l} = \frac{\partial J}{\partial a_i^l} f'\left(s_i^l\right) \tag{14}$$

As the complexity of data samples intensifies, the number of hidden layers and neurons can be increased. Through structural mapping between layers, the sample features in the original space can be mapped to a new feature space, as shown in Eq. (15) and Eq. (16), and abstract composite features can be performed at higher levels to improve the detection performance of complex data.

$$\frac{\partial J}{\partial W_{ij}^l} = \frac{\partial J}{\partial s_i^l} a_j^{l-1} \tag{15}$$

$$\delta s^l = \left(W^{l+1}\right)^T \delta s^{l+1} * f'\left(s^l\right) \tag{16}$$

The training process of deep learning models can be trained using the BP algorithm. The so-called training of neural networks refers to allowing machines to correct multiple parameters in the neural network, such as layer to layer connection weights and biases, by continuously learning the true difference information manually annotated. As shown in Eq. (17) and Eq. (18), the construction of network structures often originates from practical problems, and determining parameters requires continuous iteration to reduce the cost function in order to seek the optimal combination of network parameters. This method improves training efficiency and effectively solves the problem of local optima. Compared to traditional neural networks, RBM has no output layer and only includes visible and hidden layers, as shown in Eq. (19) and Eq. (20), while the hidden layer serves as a feature detector for extracting and learning features from the data.

$$\delta s^l = \delta A^l * f'\left(s^l\right) = \left(W^{l+1}\right)^T \delta s^{l+1} * f'\left(s^l\right) \tag{17}$$

$$\delta W^l = \frac{\partial J}{\partial W^l} = \frac{1}{m}\delta Z^l * \left(A^{l-1}\right)^T \tag{18}$$

$$N = \sum_{x \forall (circle(p))} \left| I(x) - I(p) \right| > \varepsilon_d \tag{19}$$

$$m_{pq} = \sum_{xy} x^p y^q I(x,y) \tag{20}$$

III. Differential Detection of CO2 Dense Phase Injection Model Based on Deep Confidence Networks

A. Deep Learning Theory

The training of RBM is similar to forward training, keeping the weight coefficient w of forward training unchanged [20]. At this time, the hidden layer is used as the new input for reconstruction training. The neurons of each hidden layer are multiplied by the weight, stacked, and then biased to obtain the reconstructed output, completing one reconstruction training. The reconstruction error will continuously decrease with the iterative training process of RBM until the error reaches its minimum value, and the parameter weights and biases are also updated [21, 22]. From this, it can be seen that the training process of RBM networks does not require manual annotation of data for supervision and guidance, and can learn advanced features of the original data. Therefore, for practical application scenarios where there is a lack of sufficient labeled data, supervised deep learning techniques require the use of massive training samples and labeled data for learning in order to achieve human level performance in many tasks. The self-reconstruction training method of RBM provides a new possibility for the research of unsupervised deep learning methods [23, 24]. The ORB algorithm is divided into two parts, feature point extraction and feature point description. Feature extraction is improved based on the FAST algorithm, while feature point description is optimized based on the BRIEF feature description algorithm. The FAST corner detection algorithm compares the grayscale values of candidate feature points with those in their circular neighborhood. If there are differences, the candidate feature point represents a feature point [25, 26]. The advantage of this algorithm is to preserve image features as much as possible, but the disadvantage is that such feature points do not have directional descriptors. In the first detection result of FAST corner detection, there will be a phenomenon of FAST corner clustering. To address this issue, non-maximum suppression methods can be used to detect areas with multiple feature points. Fig. 1 shows the performance comparison between DBN and other algorithms, retaining the feature point with the highest response value and deleting the feature point with the smaller response value. Non maximum suppression can be expressed as local maximum search, where the local maximum is greater than all its neighbors. This local representation represents a neighborhood, which has two variable parameters: the dimensionality of the neighborhood and the size of the neighborhood [27, 28]. Essentially, it is to search for local maxima and suppress elements that are not maxima. Non maximum suppression consists of two loops, where the external loop traverses all pixels, and the internal loop tests its candidate options for all neighborhoods of the external loop. Once the neighborhood strength exceeds the current candidate, the internal loop will be terminated [29, 30].

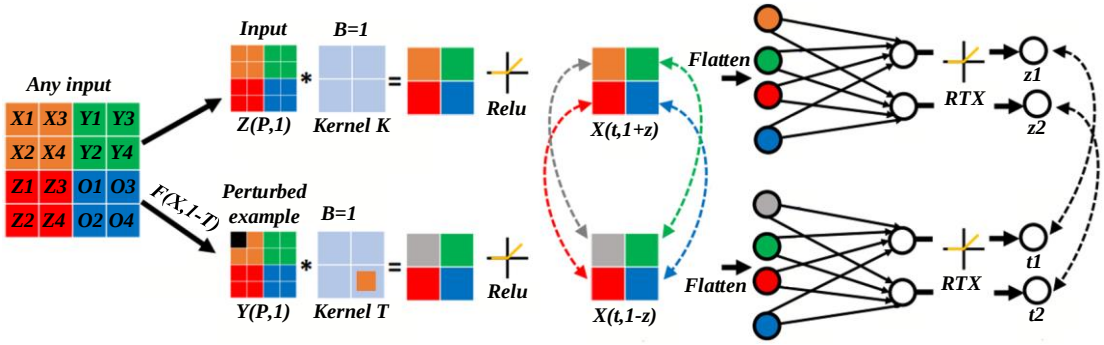

Fig. 1. Performance comparison between DBN and other algorithms.

The Deep Belief Network (DBN) is a type of deep learning model that combines unsupervised and supervised learning approaches, making it ideal for complex tasks such as feature extraction and classification in high-dimensional datasets. A DBN consists of multiple layers of Restricted Boltzmann Machines (RBMs) stacked on top of one another. Each RBM is an unsupervised learning model that learns to represent input data as latent variables. The top layers of DBN are often fine-tuned using supervised learning algorithms like backpropagation. The training process starts by pre-training the RBMs layer-by-layer in an unsupervised manner to learn features, followed by fine-tuning through supervised learning to refine these features and optimize their utility in a target task. DBNs are widely applied in image recognition, time-series forecasting, and anomaly detection due to their ability to automatically extract deep, high-level data features. In the context of carbon dioxide dense phase injection, the DBN algorithm can play a critical role in modeling and optimizing the injection process. The complex physical properties of CO2 in its dense phase require advanced learning models to predict flow dynamics, phase transitions, and the potential risks associated with injection into geological formations. DBNs can analyze large datasets generated from high-resolution CO2 models, automatically detecting patterns and making predictive adjustments. Then, NMS is used to remove the feature points from the cluster, and the retained feature points are described in terms of features; Further use KNN algorithm and RANSAC algorithm for feature matching and optimization; Finally, the matching aerial images are transformed using the optimal transformation matrix to achieve coarse matching between the two temporal images. Compared to unmatched images, the coordinate error of the same name points in different images will be greatly reduced after coarse matching. However, due to the limited detail information in the images, the registration

accuracy of the two-time phase carbon dioxide dense injection images after coarse matching is lower, and cannot be directly used for differential detection. Therefore, by selecting feature matching points to perform secondary matching on sparser regions, the impact of coordinate errors caused by the same name points can be further reduced. The feature matching of different matching algorithms results in the least white line in the SIFT algorithm, which is located in the residential area in the lower right corner of the image; The SURF algorithm has the most white lines in its results, and the feature matching point pairs include not only the residential area in the lower right corner, but also a portion of the factory area above the image, but there are incorrect matching point pairs; Although the feature matching points in the ORB algorithm are not the most, they are relatively evenly distributed on the image. Fig. 2 shows the relationship between model prediction accuracy and training rounds, and there are no incorrect matching point pairs. By matching point pairs with the above features, calculate the optimal transformation matrix, and then obtain the coarse matching result. Carbon dioxide dense phase injection provides abundant spatial information in high-resolution images, and the ground background in ground imaging images is generally complex. Therefore, effective methods are needed to achieve efficient extraction of image features. Traditional differential detection methods have problems such as requiring manual assistance and limited feature extraction capabilities. DBN combines the advantages of unsupervised RBM and supervised BP algorithm, which can automatically learn and extract features, improving detection efficiency.

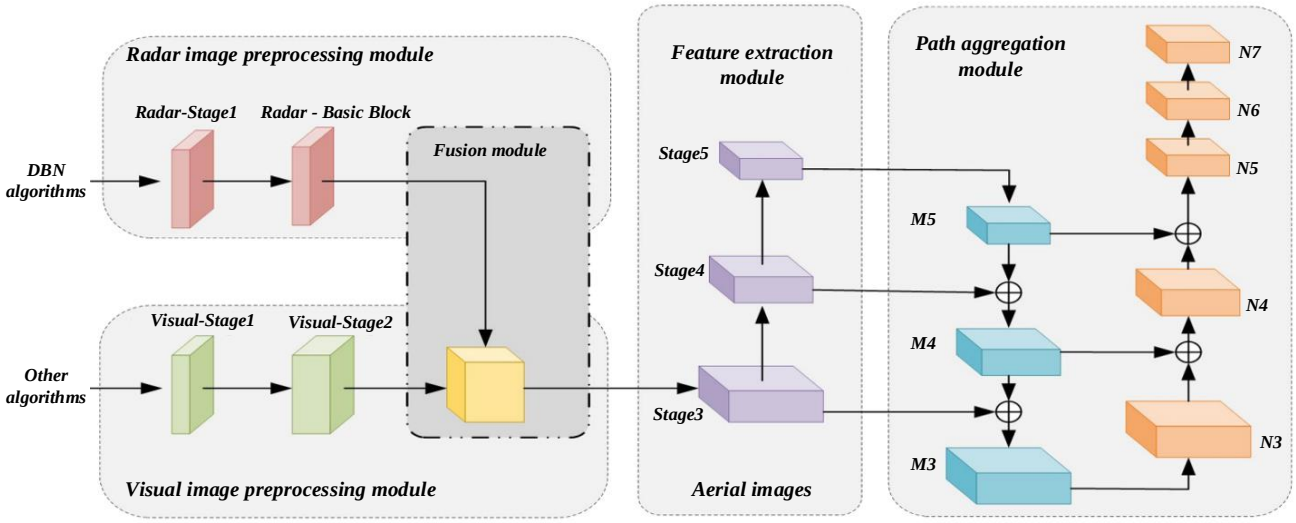

Fig. 2. Relationship between model prediction accuracy and training rounds.

B. Registration Algorithm for CO2 Dense Phase Injection Model Based on Quadratic Matching

Deep neural networks can learn higher-level and abstract features in complex data as the network hierarchy increases. Hinton et al. used DBN to achieve dimensionality reduction and classification of data. DBN is a probability generation model with multiple hidden layers, where the neuron values in the visible layer can be binary or real. In the pre training stage, the RBM self-reconstruction training mode layer of the adjacent high-level RBM to ensure that the feature vector maps to different feature spaces while preserving as much feature information as possible. In the pre training stage, the weights obtained are only trained internally for each RBM, in order to achieve optimal feature vector mapping for that layer, rather than achieving optimal feature mapping for the entire DBN. Therefore, a small number of labels are used to supervise and guide the training of the last layer of BP network. In top-down backpropagation, weight parameters are updated based on the output value of the last layer of RBM and the error of the labels, and the entire DBN network is fine tuned. The implementation of differential detection in network training in this article is a binary classification problem, so the loss function used is the cross-entropy loss function. The high-resolution carbon dioxide dense phase injection model has complex scenes and rich features, which require the extraction of effective image features for analysis. Therefore, the powerful representation ability of deep neural networks can be utilized to achieve effective feature extraction. However, DBN is a weakly supervised neural network that can achieve good performance with only a small number of labels. Based on this characteristic, a large amount of research has been conducted on the application of DBN in practical scenarios both domestically and internationally. Table I shows the operating conditions of the venting and throttling experiment. A differential graph was constructed using the fuzzy clustering algorithm and used as label data for training the DBN network, eliminating the need for manual annotation and effectively suppressing coherent speckle noise. Good results were achieved on multiple sets of SAR images.

TABLE I. OPERATING CONDITIONS FOR VENTING AND THROTTLING EXPERIMENTS

Gas composition	Gas-liquid ratio	Initial pressure in front of the valve	Temperature before throttling	Post valve pressure
100%CO_2	Infinity	1.88	18.73	0.1
100%CO_2	10	1.9	18.82	0.1
100%CO_2	1260	1.52	19.55	0.1
100%CO_2	1530	4.06	18.51	0.1

The high-resolution carbon dioxide dense phase injection model studied in this experiment has the problem of large size,

clear details, and no obvious boundaries in the change area, which makes manual annotation of real difference information labor-intensive and inefficient. Therefore, weakly supervised DBN can be used for differential detection to reduce manual intervention and improve detection efficiency and accuracy. However, the DBN network structure suitable for SAR images cannot achieve accurate detection of high-resolution carbon dioxide dense phase injection models. Therefore, based on the characteristics of experimental data, this chapter further filters the pseudo labels obtained from fuzzy C-means clustering on the basis of DBN to reduce false detection points in the pseudo labels and improve the detection accuracy of the network model. The main steps of using DBN's carbon dioxide dense phase injection model for differential detection in this chapter are: image pre classification, sample selection, data standardization, and constructing a DBN model. Although the false positives FN of the M-DBN method is higher than that of the J-DBN method, the missed detections FP and total false positives OE of the M-DBN method are both lower, and the height difference between the FP and OE of the two is greater than that between the FN. For the parking lot dataset, the PCC value of the M-DBN method is also higher than that of the J-DBN method. Compared to J-DBN, the Kappa coefficient of the M-DBN method reached 90.6%, the Jaccard coefficient increased by 8%, and the YC value increased by about 12 percentage points. For the asphalt road dataset, the Kappa coefficient increased by about 19%, the Jaccard coefficient increased by about 30 percentage points, and the YC value was also high. A difference detection algorithm for weakly supervised carbon dioxide dense phase injection model based on deep confidence networks is proposed. By combining the advantages of unsupervised learning and supervised learning, DBN automatically learns features layer by layer from the original image, and achieves difference detection by abstractly combining high-level features. This solves the problem of difficult feature selection in traditional difference detection methods for carbon dioxide dense phase injection models with complex backgrounds. Fig. 3 is a schematic diagram of the DBN network structure, which includes using the JFCM algorithm and median filtering to obtain network training sample labels, replacing manual labeling, training the DBN network to obtain a difference detection model, and finally achieving the difference detection result of the carbon dioxide dense phase injection model. Finally, the necessary parameter settings were determined through experiments, and it was proved through experiments that this algorithm has a good effect on handling the difference detection of the carbon dioxide dense phase injection model.

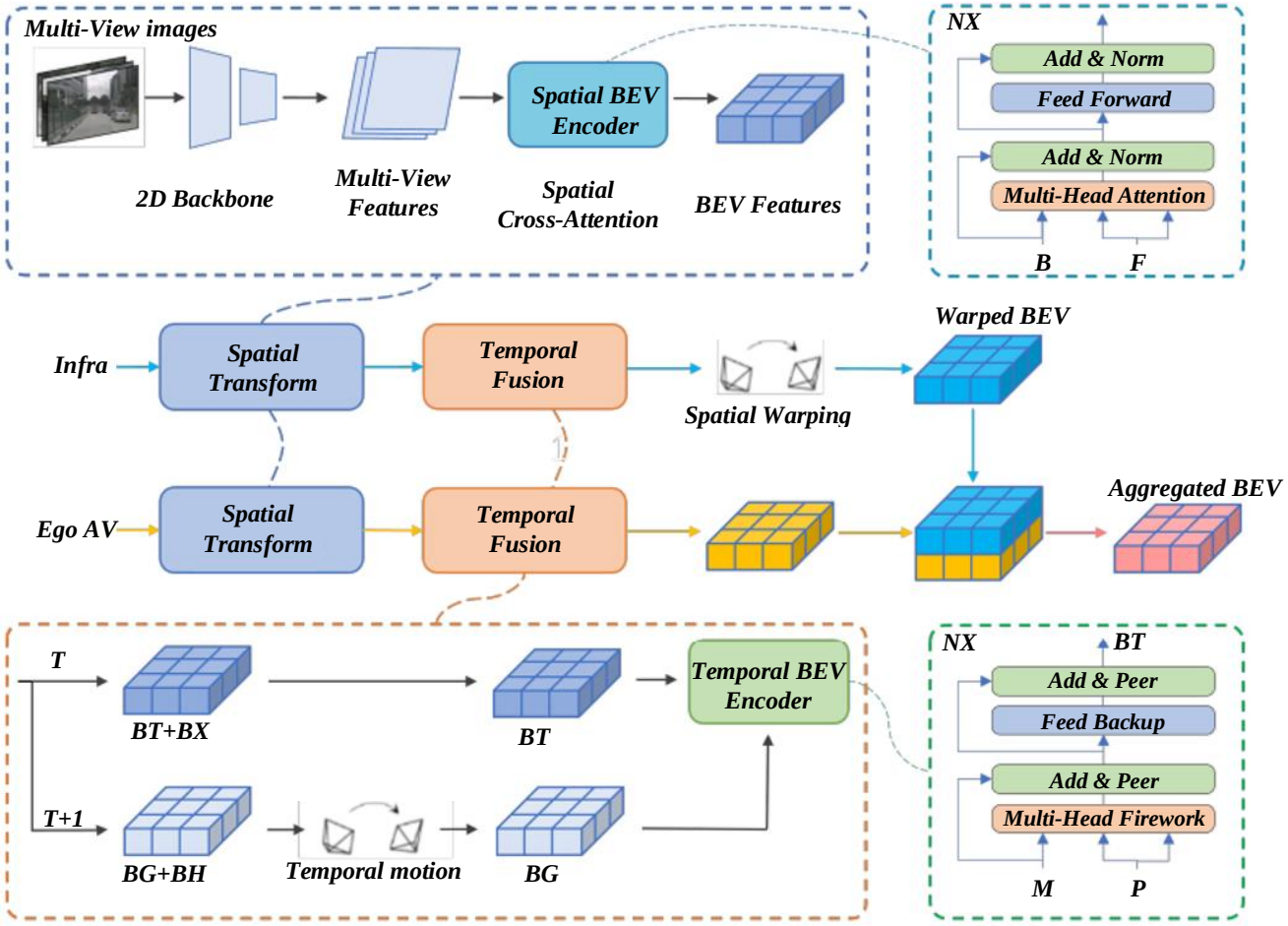

Fig. 3. Schematic diagram of DBN network structure.

IV. Optimization of CO2 Dense Phase Injection Model Based on DBN Deep Learning Algorithm

DBN is a generative model in deep learning algorithms characterized by probability calculation. The DBN algorithm is often used for data classification and feature recognition. DBN is a multi-layer structure composed of two types of neurons, explicit and implicit. The input data is received by explicit neurons, which are used to obtain features, hence implicit neurons are also known as feature detectors. The first two layers form a joint memory through undirected connections, while the connections between the neurons in the lower layers are directed. The lowest layer forms a data vector, where a single neuron represents one dimension. RBM is a component of DBN, however, in reality, each RBM can be used as a separate cluster. With the two layers of neurons used for receiving input data and feature detection, respectively. Fig. 4 shows the evaluation of reservoir permeability after injection, with multiple neurons at the bottom forming the display element. Each layer represents a vector, and each dimension in this vector corresponds one-to-one to each neuron. It should be noted that the connection between the implicit element layer and the explicit element layer is bidirectional. Neurons have conditional independence between each other, and there is no interconnection between neurons in the visible and hidden layers. Only neurons between layers have symmetrical connecting lines.

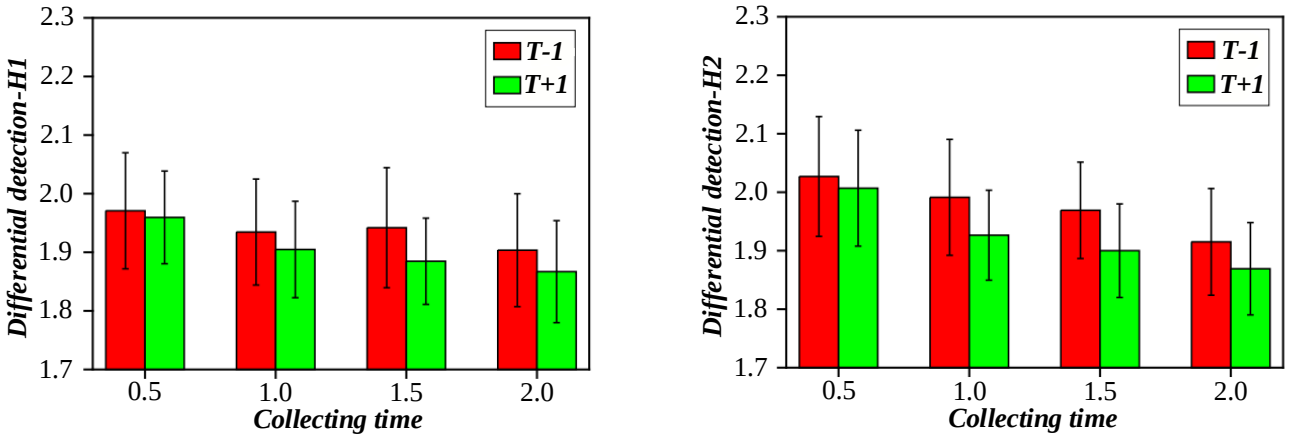

Fig. 4. Evaluation of reservoir permeability after injection.

Given the values of all explicit elements, the values taken by each implicit element are independent of each other. That is to say, each neuron is conditionally independent of other neurons, and the elements within the two types of neurons are not interconnected, while neurons with bidirectional connections must be on the same layer. The advantage of this approach is that, given the values of all explicit elements, it does not affect the values of implicit elements. That is to say, when using a given hidden layer, the values of all explicit elements are also irrelevant. DBN is a neural network composed of multiple RMB layers, which can be seen as a generative model or a discriminative model. Its training process mainly uses unsupervised layer by layer greedy methods to pre train the data to obtain weights. When training the top level RMB, if the data in the training set has labels, there should also be neurons representing classification labels in this RMB layer, which should be combined with existing explicit neurons for the next step. Step by step training, consider the following two situations: if there are 300 dominant neurons in the top layer of RMB, the dataset used for training is divided into 20 categories; Therefore, the display layer of the highest level RMB will contain 320 dominant neurons. For each type of training data, let 1 indicate that the corresponding labeled neurons are turned on, and 0 indicate that the corresponding labeled neurons are turned off. Table II compares the SIFT, SURF, and ORB algorithms. Except for the top-level RMB, the weights of RMB at other levels are divided into two categories: upward cognitive weights and downward generative weights.

TABLE II. Comparison of SIFT, SURF, and ORB Algorithms

Algorithm	Number of feature points	Optimal matching pair	Time (seconds)
Sift	9342	51	86.85
Surf	2625	200	21.26
Orb	6428	108	5.98

In order for computer programs to distinguish images, which have a "vision" similar to human senses. Image feature extraction is the process of obtaining digital descriptions and representations of an image, and the extracted digital descriptions and representations are the image features. These digitized features can be in numerical or vector form. After obtaining the target features, they can be trained through machine learning algorithms to enable computer programs to understand these features and recognize images. Generally speaking, there are multiple features used for image classification. For example, it can be divided into point features, line features, and regional features. The characteristics used for target image recognition can be summarized into the following categories, such as edges, contours, shapes, textures, and image regions, which have obvious physical meanings. It is divided into grayscale histogram features and moment features. Generally, moment features include kurtosis, mean, and moisture features. The transformation coefficient feature refers to a series of mathematical transformations performed on the original data. Algebraic features indicate a certain algebraic property of an image. From the perspective of mapping, data

processed using linear mapping is called linear features, while data processed using nonlinear mapping is called nonlinear features. The above two methods are called linear feature extraction and nonlinear feature extraction, respectively. Among them, linear feature extraction methods are widely used. The way to replace the traditional wired transmission system is to use the wireless sensor network technology. The wireless sensor network is a distributed sensor network. Its end is a sensor that can sense and check the external world. Fig. 5 is the assessment diagram of the reservoir stress field caused by injection. The sensors in the network communicate through wireless means.

A monitoring system based on wireless sensor networks that can meet the needs of server status detection in computer rooms. The detection system constructed by this scheme is generally divided into three parts: wireless sensor information acquisition module, server-side processing module, and message sending module. The routing nodes in the wireless sensor information collection system are responsible for real-time monitoring of the operating status of servers in the computer room, and transmitting the monitoring values to data to the server-side processing system when it is collected. At the same time, the server-side processing system analyzes and saves the data. Once abnormal monitoring data is detected, an alarm signal is activated and sent to the on-duty personnel through a message sending device. If there are no abnormal situations, the server-side system can regularly send the collected data to users via SMS. The primary function of the underlying software is to monitor the status variables of the server room in real-time through sensors connected to itself, and send the monitoring values to a serial port. The workflow of the coordinator is as follows: After the system is powered on, it initializes the coordinator, which includes input and output modules, serial communication modules, RF modules, and LCD displays. Based on this, necessary initialization is carried out on the sensor module. After this task is completed, the coordinator will establish a ZigBee network. Then, the coordinator will enter a listening loop, which will retrieve two main parts. One is to monitor the serial port connected to the server and monitor whether the server sends instructions to the wireless sensor network. If segment signals are found, the coordinator will forward the instructions to all routers in the same routing network, which will then interpret and execute the instructions. Fig. 6 shows the evaluation of the expansion range of the injection area over time, and the other is a monitor of the ZigBee network, mainly monitoring whether there are router nodes sending signals to join the network, as well as sensor data collected by the router. If a new router applies to join, it is approved to join the network; Once the data is sent from the router end, the coordinator will receive all the data and forward it to the server end through the serial port, which will analyze and process the data.

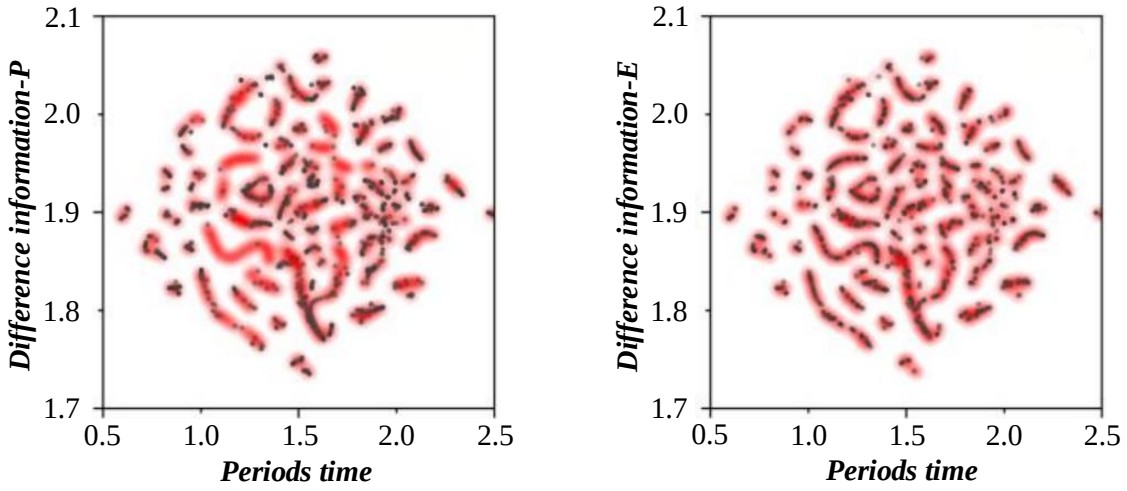

Fig. 5. Evaluation of reservoir stress field caused by injection.

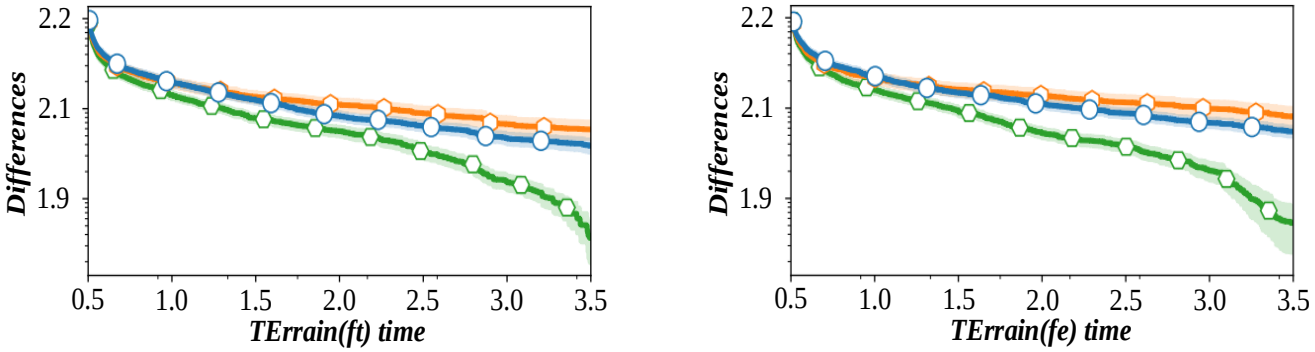

Fig. 6. Evaluation graph of injection region expansion range over time.

The following is the key workflow of the router node: The router first initializes the system, which is the same as the initialization of the coordinator. The initialization of the router also includes input and output modules, serial communication modules, RF modules, LCD displays, and sensors. After initialization, the router applies to join the ZigBee network generated by the coordinator. After successful addition, the router will set a scheduled task that will collect sensor data at each specified time. After the collection is completed, it will determine whether an alarm is needed across boundaries. If so, the alarm device will be immediately activated. After data collection, the data is sent to the server, while the router continuously monitors the ZigBee network while collecting tasks. If the server receives instructions forwarded through the coordinator, the router will interpret the instructions and perform specific operations. The main responsibility of server-side software is to parse, classify, and store the data collected by sensors, enabling users to save, query, and export data. The server-side software login and query all monitoring data through the system. At the same time, the system is also connected to the SMS sending device, and at each fixed time, the system will send monitoring data to users through the SMS sending device. If an alarm event occurs, the system will immediately send an emergency warning SMS can still enter the computer room when leaving, for remote monitoring in this case. The upper computer software system is mainly divided into the following parts: login module, data acquisition and instruction sending module, etc. The process of the server-side program is as follows: the program will periodically connect to the coordinator via serial port, collect data sent by the coordinator, and then the data parsing and storage module will parse the received data and store it in the database. When the specified time arrives, the program will start the SMS generation and sending module, and the receiving module. The collected data is sent to users through SMS sending devices. Fig. 7 shows the evaluation of reservoir pore volume utilization rate. Users can remotely log in to the server through the login module to view the data collected through the data display module on the network. Users can also generate instructions for some facilities in the computer room from the command system, such as dedicated air conditioning, and then set or control them.

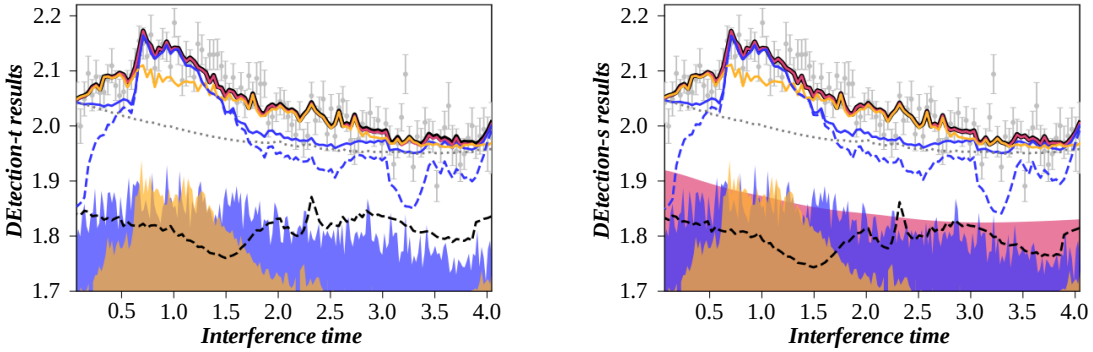

Fig. 7. Evaluation of reservoir pore volume utilization efficiency.

V. Experimental Analysis

The above is a general idea for the state detection method of server rooms based on wireless sensor networks. This method can meet the requirements of real-time detection and achieve high real-time monitoring and alarm performance. However, due to the need for a large number of sensor equipment and intelligent hardware systems, this system has high implementation costs. Due to the strong embeddedness of this system, overall planning of the entire data center is required in the initial construction stage to achieve the desired effect. Fig. 8 shows the evaluation of injection efficiency and injection pressure, so it is not suitable for data centers that have already been built and put into use.

However, the limitations of pixel level image fusion cannot be ignored. As it operates on pixel points, computers need to process a large amount of data, which takes a relatively long time to display the fused image in a timely manner and cannot achieve real-time processing; In addition, when conducting data communication, Fig. 9 shows the dynamic evaluation of reservoir fluids. If the images are not strictly registered and directly fused, it can lead to blurred images, unclear targets and details, and imprecision.

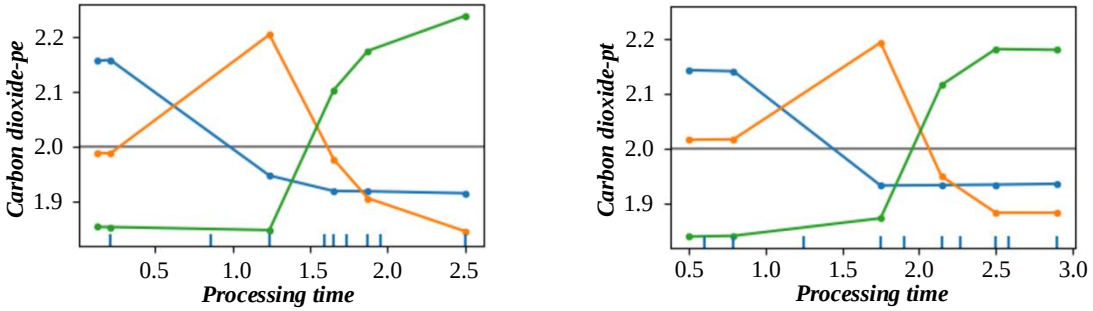

Fig. 8. Evaluation chart of injection efficiency and injection pressure.

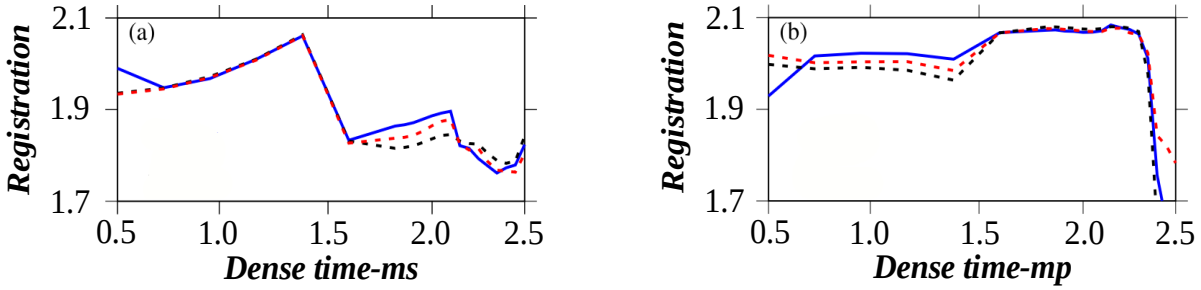

Fig. 9. Reservoir fluid dynamic evaluation diagram.

Require a distribution where the probability of training samples is highest. Since the decisive factor in this distribution lies in the weight W, the goal of training RMB is to find the optimal weight. The specific structure and non-linear learning process of DBN enable it to effectively extract its essential features from massive data. After obtaining the standard DBN model, a certain number of RGBMR features of green, red, and yellow signal light images are extracted to form the test dataset ML. Fig. 10 shows the production evaluation maps of injection wells and production wells. The ML is input into the standard DBN model trained in this section for evaluation and classification, and the signal light status of each corresponding image for each set of data can be identified.

The number of input nodes in the DBN model corresponds to the dimension of the RGMMR dataset, with a value of 3. Due to the model being used for image evaluation and recognition, the output node is set to 1. Fig. 11 shows the evaluation of carbon dioxide saturation profile. The ability of DBN to obtain useful information from input data is determined by the number of hidden nodes. Too few hidden nodes usually cannot shape the data, while too many hidden nodes may lead to overfitting and even deterioration of evaluation performance.

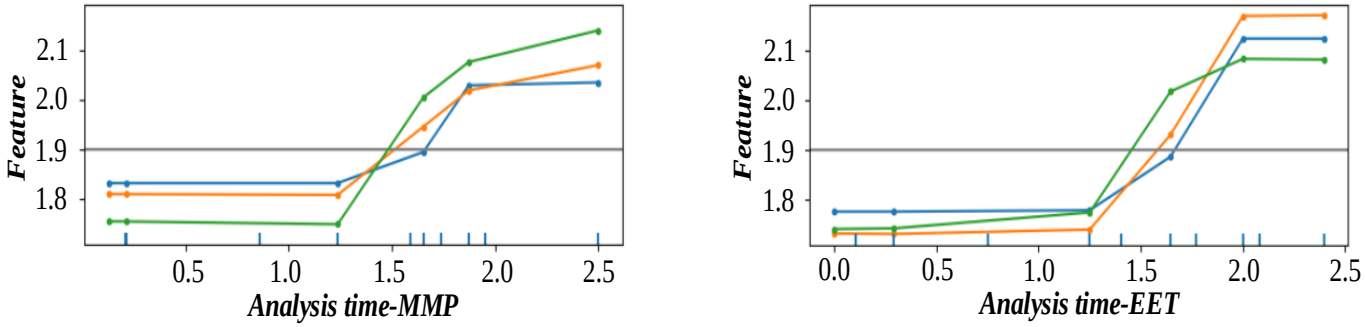

Fig. 10. Production evaluation of injection and production wells.

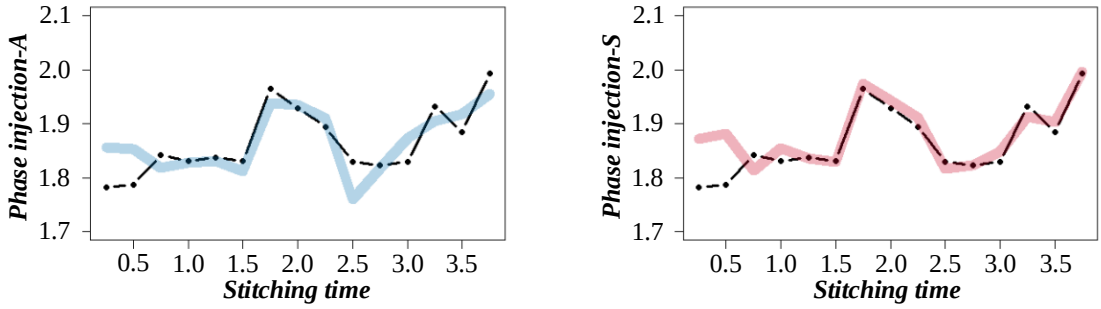

Fig. 11. Evaluation of carbon dioxide saturation profile.

VI. Conclusion

Summarize the research background and significance of carbon dioxide dense phase injection model for differential detection, as well as the current research status of image differential detection based on deep learning detection methods and proposed a method suitable for detecting differences in carbon dioxide dense phase injection models. In response to the large amount of data in high-resolution aerial images, which leads to low matching efficiency and longtime consumption of traditional registration algorithms, this paper proposes a registration method based on a secondary matching CO2 dense phase injection model. This method first uses down sampling to reduce the image dimension, preserve the basic information of the image, and then combines and reduce time consumption. The implementation of the DBN deep learning model facilitated a

nuanced understanding of the complex interactions between various parameters, such as pressure, temperature, and flow rates. Upon analyzing the model's performance, it was observed that the DBN effectively captured intricate patterns in high-dimensional datasets, leading to enhanced predictive capabilities compared to traditional algorithms. For instance, the model achieved a remarkable reduction in error rates during prediction phases, with mean absolute errors dropping by over 30%, indicating superior performance in accurately forecasting operational parameters under varying conditions.

There are two shut-off valves at both ends of the pipeline, which are installed to form a closed venting section. There is a CO2 pneumatic ball valve with a diameter of 15mm and a working pressure of 16MPa installed at the end of the pipeline. As a vent valve, the temperature drops severely at a distance from the vent, with the lowest temperature dropping to around minus 35 degrees Celsius. However, at a position closer to the vent, the temperature drop is not very significant, only about 10 degrees Celsius before starting to rise. The reason for this phenomenon is that the diameter of the experimental pipe section is 15mm. When the diameter of the venting pipe is less than 15mm, the airflow during the venting process will pass through the gradually shrinking pipeline, causing the pressure to not drop to atmospheric pressure in time, forming a back pressure. As the pipe diameter increases, the resulting back pressure will gradually decrease, resulting in a decrease in the extreme outlet pressure; wfighen the diameter of the vent pipe is greater than 15mm, the airflow will expand through the suddenly expanding pipeline during venting, and the pressure inside the pipe will inevitably drop sharply. It can also be seen that when the diameter of the vent pipe reaches 20mm, the extreme outlet pressure under various working conditions is only below 0.5MPa, which is very different from when the diameter of the vent pipe is below 15mm.

REFERENCES

[1] Bharadwaj Neeraj, Ballings Michel, Naik Prasad A., Moore Miller & Arat Mustafa Murat. (2022). A New Livestream Retail Analytics Framework to Assess the Sales Impact of Emotional Displays. Journal of Marketing (1), 27-47.

[2] Gao Bin, Zhou Jiazheng, Yang Yuying, Chi Jinxin & Yuan Qi. (2022). Generative adversarial network and convolutional neural network-based EEG imbalanced classification model for seizure detection. Biocybernetics and Biomedical Engineering (1), 1-15.

[3] Hu Zhongyang, Kuipers Munneke Peter, Lhermitte Stef, Izeboud Maaike & van den Broeke Michiel. (2021). Improving surface melt estimation over the Antarctic Ice Sheet using deep learning: a proof of concept over the Larsen Ice Shelf. The Cryosphere(12),5639-5658.

[4] Gan Jiaan, Shen Mengyan, Xiao Xin, Nong Jinpeng & Feng Fu. (2021). Deep learning enables temperature-robust spectrometer with high resolution. Optoelectronics Letters (12), 705-709.

[5] Geiss Andrew & Hardin Joseph C. (2021). Inpainting radar missing data regions with deep learning. Atmospheric Measurement Techniques (12), 7729-7747.

[6] Wang Zhichao, Xia Hong, Zhu Shaomin, Peng Binsen, Zhang Jiyu, Jiang Yingying & Annor Nyarko M. (2022). Cross-domain fault diagnosis of rotating machinery in nuclear power plant based on improved domain adaptation method. Journal of Nuclear Science and Technology (1), 67-77.

[7] Lamba Monika, Gigras Yogita & Dhull Anuradha. (2021). Classification of plant diseases using machine and deep learning. Open Computer Science (1), 491-508.

[8] Xue Bin, Xu Zhong bin, Huang Xing & Nie Peng cheng. (2021). Data-driven prognostics method for turbofan engine degradation using hybrid deep neural network. Journal of Mechanical Science and Technology (12), 5371-5387.

[9] Hu Hao, Zhang Chao & Liang Yanxue. (2021). Detection of surface roughness of mechanical drawings with deep learning. Journal of Mechanical Science and Technology (12), 5541-5549.

[10] Abbas Ather, Baek Sangsoo, Silvera Norbert, Soulileuth Bounsamay, Pachepsky Yakov, Ribolzi Olivier & Cho Kyung Hwa. (2021). In-stream Escherichia coli modeling using high-temporal-resolution data with deep learning and process-based models. Hydrology and Earth System Sciences (12), 6185-6202.

[11] Wu Xueshan, Huang Song, Li Min & Deng Yufeng. (2021). Vector Magnetic Anomaly Detection via an Attention Mechanism Deep-Learning Model. Applied Sciences(23),11533-11533.

[12] Hussain Rukhshanda, Karbhari Yash, Ijaz Muhammad Fazal, Woźniak Marcin, Singh Pawan Kumar & Sarkar Ram. (2021). Revise-Net: Exploiting Reverse Attention Mechanism for Salient Object Detection. Remote Sensing (23), 4941-4941.

[13] Fauvel Kevin, Lin Tao, Masson Véronique, Fromont Élisa & Termier Alexandre. (2021). XCM: An Explainable Convolutional Neural Network for Multivariate Time Series Classification. Mathematics(23),3137-3137.

[14] Li Xiao, Ning Huan, Huang Xiao, Dadashova Bahar, Kang Yuhao & Ma Andong. (2022). Urban infrastructure audit: an effective protocol to digitize signalized intersections by mining street view images. Cartography and Geographic Information Science (1), 32-49.

[15] Xie Yuting, Chi Xiaowei, Li Haiyuan, Wang Fuwen, Yan Lutao, Zhang Bin & Zhang Qinjian. (2021). Coal and Gangue Recognition Method Based on Local Texture Classification Network for Robot Picking. Applied Sciences (23), 11495-11495.

[16] Park Hyun Joon, Lee Min Seok, Park Dong Il & Han Sung Won. (2021). Time-Aware and Feature Similarity Self-Attention in Vessel Fuel Consumption Prediction. Applied Sciences (23), 11514-11514.

[17] Chen Yanming, Liu Xiaoqiang, Xiao Yijia, Zhao Qiqi & Wan Sida. (2021). Three-Dimensional Urban Land Cover Classification by Prior-Level Fusion of LiDAR Point Cloud and Optical Imagery. Remote Sensing(23),4928-4928.

[18] Xu Lei, Zheng Shunyi, Na Jiaming, Yang Yuanwei, Mu Chunlin & Shi Debin. (2021). A Vehicle-Borne Mobile Mapping System Based Framework for Semantic Segmentation and Modeling on Overhead Catenary System Using Deep Learning. Remote Sensing (23), 4939-4939.

[19] Dong Sunghee, Jin Yan, Bak SuJin, Yoon Bumchul & Jeong Jichai. (2021). Explainable Convolutional Neural Network to Investigate Age-Related Changes in Multi-Order Functional Connectivity. Electronics(23),3020-3020.

[20] Chen Guanzhou, Tan Xiaoliang, Guo Beibei, Zhu Kun, Liao Puyun, Wang Tong... & Zhang Xiaodong. (2021). SDFCNv2: An Improved FCN Framework for Remote Sensing Images Semantic Segmentation. Remote Sensing(23),4902-4902.

[21] Wu Weichao, Xie Zhong, Xu Yongyang, Zeng Ziyin & Wan Jie. (2021). Point Projection Network: A Multi-View-Based Point Completion Network with Encoder-Decoder Architecture. Remote Sensing(23), 4917-4917.

[22] Mirzaei Majid, Yu Haoxuan, Dehghani Adnan, Galavi Hadi, Shokri Vahid, Mohsenzadeh Karimi Sahar & Sookhak Mehdi. (2021). A Novel Stacked Long Short-Term Memory Approach of Deep Learning for Streamflow Simulation. Sustainability (23), 13384-13384.

[23] Valls Canudas Núria, Calvo Gómez Míriam, Golobardes Ribé Elisabet & Vilasis Cardona Xavier. (2021). Use of Deep Learning to Improve the Computational Complexity of Reconstruction Algorithms in High Energy Physics. Applied Sciences (23), 11467-11467.

[24] Hur Yuna, Son Suhyune, Shim Midan, Lim Jungwoo & Lim Heuiseok. (2021). K-EPIC: Entity-Perceived Context Representation in Korean Relation Extraction. Applied Sciences (23), 11472-11472.

[25] Alkassar Sinan, Abdullah Mohammed A. M., Jebur Bilal A., AbdulMajeed Ghassan H., Wei Bo & Woo Wai Lok. (2021). Automated Diagnosis of Childhood Pneumonia in Chest Radiographs Using Modified Densely Residual Bottleneck-Layer Features. Applied Sciences (23), 11461-11461.

[26] Jiang Gangwu, Sun Yifan & Liu Bing. (2021). A fully convolutional network with channel and spatial attention for hyperspectral image classification. Remote Sensing Letters (12), 1238-1249.

[27] Li Mingxiao, Gao Song, Lu Feng, Liu Kang, Zhang Hengcai & Tu Wei. (2021). Prediction of human activity intensity using the interactions in physical and social spaces through graph convolutional networks. International Journal of Geographical Information Science(12),2489-2516.

[28] Park Hyebin & Lim Yujin. (2021). Deep Reinforcement Learning Based Resource Allocation with Radio Remote Head Grouping and Vehicle Clustering in 5G Vehicular Networks. Electronics (23), 3015-3015.

[29] Alqahtani Ali, Ali Mohammed, Xie Xianghua & Jones Mark W. (2021). Deep Time-Series Clustering: A Review. Electronics (23), 3001-3001.

[30] Castro Tapia Salvador, CastañedaMiranda Celina Lizeth, OlveraOlvera Carlos Alberto, Guerrero Osuna Héctor A., OrtizRodriguez José Manuel, MartínezBlanco Ma. del Rosario... & SolísSánchez Luis Octavio. (2021). Classification of Breast Cancer in Mammograms with Deep Learning Adding a Fifth Class. Applied Sciences (23), 11398-11398.